UCRL-11892

University of California

Ernest O. Lawrence Radiation Laboratory

TWO-WEEK LOAN COPY

This is a Library Circulating Copy which may be borrowed for two weeks. For a personal retention copy, call Tech. Info. Division, Ext. 5545

MUON POLARIZATION AND ENERGY SPECTRUM IN $K^+ \rightarrow \pi^0 + \mu^+ + \nu$

Berkeley, California

DISCLAIMER

This document was prepared as an account of work sponsored by the United States Government. While this document is believed to contain correct information, neither the United States Government nor any agency thereof, nor the Regents of the University of California, nor any of their employees, makes any warranty, express or implied, or assumes any legal responsibility for the accuracy, completeness, or usefulness of any information, apparatus, product, or process disclosed, or represents that its use would not infringe privately owned rights. Reference herein to any specific commercial product, process, or service by its trade name, trademark, manufacturer, or otherwise, does not necessarily constitute or imply its endorsement, recommendation, or favoring by the United States Government or any agency thereof, or the Regents of the University of California. The views and opinions of authors expressed herein do not necessarily state or reflect those of the United States Government or any agency thereof or the Regents of the University of California.

Submitted to Phys. Rev.

UCRL-11892

UNIVERSITY OF CALIFORNIA
Lawrence Radiation Laboratory
Berkeley, California

AEC Contract No. W-7405-eng-48

MUON POLARIZATION AND ENERGY SPECTRUM IN $K^+ \rightarrow \pi^0 + \mu^+ + \nu$

D. Cutts, T. Elioff, and R. Stiening

January 1965

11592

Muon Polarization and Energy Spectrum in $K^+ \rightarrow \pi^o + \mu^+ + \nu$

D. Cutts, T. Elioff, and R. Stiening

Lawrence Radiation Laboratory, Berkeley*

ABSTRACT

The number of muons in the high energy region of the continuum in the reaction $K^+ \rightarrow \pi^o + \mu^+ + \nu$ has been measured. The portion of the spectrum explored extended from 107.1 to 126.4 MeV. We measured the longitudinal polarization of the muons in the same energy interval by observing the spatial anisotropy of the e^+ from muon decay. The rate of decay with a muon in this energy interval was found to be 0.054 ± 0.008 of the total K^+ decay rate in the mode $K^+ \rightarrow \pi^o + e^+ + \nu$. The polarization of the muons was found to be +0.61 ± 0.39. These results are consistent with an analysis made assuming constant form factors, pure vector coupling, and equal muon and electron weak coupling strength. A real or imaginary vector form factor ratio, $\xi = \frac{f-}{f+}$, is consistent with the data. If ξ is real, the most probable solution is $+0.2 < \xi < +1.4$. As a calibration experiment, we measured the polarization of muons from $K^+ \rightarrow \mu^+ + \nu$. We found it to be -0.94 ± 0.21.

*Work performed under the auspices of the U. S. Atomic Energy Commission

INTRODUCTION

The central idea of the present theory of weak interactions is that the Hamiltonian density can be written as the product of a current with itself.

$$H = \sum_{\lambda} J_{\lambda}^{*} J_{\lambda} \tag{1}$$

The current J_{λ} is thought of as being the sum of a number of contributions.

$$J_{\lambda} = J_{\lambda}^{\ell} + J_{\lambda}^{s,\Delta s=0} + J_{\lambda}^{s,\Delta s=1} + \cdots \tag{2}$$

In this picture the various observed weak processes arise from different terms in the product $\sum J^{*}J$.

From nuclear beta decay, muon decay, and pion decay, the structure of the leptonic current term in the above sum has been established.

$$J_{\lambda}^{\ell} = \frac{G}{\sqrt{2}} \left[\bar{U}_{\mu}\gamma_{\lambda}(1+\gamma_5)U_{\nu,\mu} + \bar{U}_{e}\gamma_{\lambda}(1+\gamma_5)U_{\nu,e} \right] \tag{3}$$

It is essential to the above theory that the form of J_{λ}^{ℓ} be that given above in all processes in which J_{λ}^{ℓ} appears. One test of this is the coupling of J_{λ}^{ℓ} to the current of strongly interacting particles which changes strangeness, $J_{\lambda}^{s,\Delta s=1}$. It is known that weak decays which change strangeness are slower than those which do not change strangeness. The question then arises whether the structure of the weak coupling is different in the processes which change strangeness.

The process that has been chosen to study this coupling is the $K^{+} \rightarrow \pi^{0} + \mu^{+} + \nu$ decay. By measuring the energy spectrum as well as the polarization of the muons, one can determine the structure of the muonic part of the weak current J_{λ}^{ℓ}. Furthermore, by comparing the process with the $K^{+} \rightarrow \pi^{0} + e^{+} + \nu$ decay it is possible to test the equality of coupling strength of electrons and muons which is implied by the form of J_{λ}^{ℓ}.

EXPERIMENTAL ARRANGEMENT*

A. K^+ Meson Beam

The K^+ mesons were produced by degrading to rest the K^+ mesons in and unseparated, momentum analyzed secondary particle beam produced when 5.2 BeV protons struck a three inch thick uranium target. The magnet system used for the momentum analysis of the secondary beam is shown in Fig. 1. Particles produced in a direction parallel to the incident proton beam were deflected through an angle of 35° by magnet B1. A quadrupole doublet Q1,Q2 with Q1 focussing in the horizontal plane, focussed the beam on the stopping region. Magnet B2 deflected the beam through another angle of 35°. The beam was collimated at the entrance and exit of the quadrupole doublet and in the bending magnet B2. In order to compensate for the momentum dispersion of the beam at the stopping region, part of the carbon degrader used to stop the K^+ mesons was wedge shaped. We used a counter system to separate stopping K^+ mesons from other particles in the beam. It consisted of three scintillation counters, S2,S3, and S4, in the beam degrader, with discriminators set to require pulses greater than those produced by minimum ionizing particles, and a water Cerenkov counter in anticoincidence to reject fast particles. There were two scintillation counters, S6 and S6B,in which the K^+ mesons stopped, and a scintillation counter, S7, in anticoincidence to reject particles passing through the entire telescope.

A typical magnet tuning curve is shown in Fig. 2. The rate at which K^+ mesons could be stopped was limited by the background in the spark chambers caused by the interactions of π^+ mesons in the beam with the degrader. The momentum of the beam was set to maximize the ratio of stopping K^+ mesons to π^+ mesons passing through the degrader. The momentum chosen

*Preliminary results of this experiment are given in the Bull. Am. Phys. Soc. 10, 91(1965)

as optimum with regard to this consideration was 470 MeV/c. In the experiment the stopping K^+ rate was about 800 particles/Bevatron pulse. Under these conditions, the π^+ rate in the counter telescope was about 400,000/pulse. The average Bevatron pulse duration was 0.6 seconds.

B. Spark Chambers and Counters

Fig. 3 shows the apparatus used to detect K^+ decays. An acceptable event occurred when a K^+ came to rest in either counter S6 or S6B and decayed, giving rise to a μ^+ lepton which passed through the T2, T3, T4 counter telescope and came to rest before reaching anticoincidence counter T5. Between T2 and T4 spark chambers with copper plates degraded the muons, and permitted observation of their behavior during the degrading process. Between T4 and T5, spark chambers with plates made of 20% aluminum and 80% carbon ($\rho = 1.76$) was operated so as to be sensitive to both the stopping muon and to the positron from the muon decay provided that the decay occured within 3.3×10^{-6} seconds after the muon stopped. We measured the longitudinal polarization of the stopping muons by observing the spatial distribution of the positrons in the $\mu^+ \rightarrow e^+ + \nu + \bar{\nu}$ decays. We measured the energy distribution of the muons from K^+ decay by observing the range distribution of the muon decay vertices, or the stopping points when a decay positron was not visible. We determined the branching ratio for $K^+ \rightarrow \pi^0 + \mu^+ + \nu$ with muons in the above range interval by comparing the number of stopping muons with the number of T2, T3, T4, T5 coincidences. These later events were almost entirely due to muons from $K^+ \rightarrow \mu^+ + \nu$ events.

The range interval between T4 and T5 in which the muons came to rest was selected to be beyond the range of π^+ mesons from the decay

$K^+ \rightarrow \pi^o + \pi^+$, but less than the range of muons from the decay $K^+ \rightarrow \mu^+ + \nu$. The muon kinetic energy corresponding to the chosen range interval extended from 107 to 135 MeV. Because the rate of muons from $K^+ \rightarrow \pi^o + \mu^+ + \nu$ was small compared to other backgrounds near the high end of the range interval, only those muons with an initial kinetic energy of less than 126.4 MeV were used in the data analysis. In addition to muons from $K^+ \rightarrow \pi^o + \mu^+ + \nu$, other K^+ decay processes can give rise to particles stopping in the above described range interval.

These are:

(1) Muons from $K^+ \rightarrow \mu^+ + \nu + \gamma$.

(2) Muons from the decay in flight of pions from $K^+ \rightarrow \pi^o + \pi^+$.

(3) The decay in flight of muons from $K^+ \rightarrow \mu^+ + \nu$.

(4) Muons and pions from the decay in flight of K^+ mesons in the region of the S6, S6B stopping counters.

(5) Positrons from $K^+ \rightarrow \pi^o + e^+ + \nu$.

(6) Particles from K^+ mesons which did not come to rest in the S6, S6B stopping counter region.

The first three categories of background events could not be distinguished from $K^+ \rightarrow \pi^o + \mu^+ + \nu$ events since π^o decay gamma rays were not detected. We have accounted for the events in these two categories by calculations taking into account the K^+ decay branching ratios and the geometry of the spark chamber assembly. These calculations will be described later. Background events in the remaining three categories were eliminated by making use of the pulse height and time information from the scintillation counters, and by conditions set on the appearance of particle tracks in the spark chambers.

We utilized the pulse height and time information from the

scintillation counters in the following manner. A stopping K^+ was identified as a coincidence among counters S3, S4, S5, and S6 in anti-coincidence with a water Cerenkov counter and counter S7. Pulses were accepted from S3, S4, S5, and S6 only if the pulse height was considerably greater than that corresponding to a minimum ionizing particle. The pulse height condition on S6 was such that the minimum acceptable energy loss was 6 MeV, or more than twice the energy loss of a minimum ionizing particle. When the K^+ penetrated the S6B counter, the information was used to light a marker lamp which appeared on the spark chamber photograph if a picture was taken. This was done so that a range correction could be applied to the K^+ decay products. These criteria on the stopping K^+ beam were sufficient to eliminate most of the other particles in the unseparated beam. The background of events satisfying the above conditions but not being due to stopping K^+ mesons was less than 10% of the stopping K^+ rate.

Whenever the K^+ beam counter telescope indicated that a K^+ had stopped, a gate was opened to accept a coincidence in the T2, T3, T4 counter telescope provided that it occurred after a certain time delay. This delay was chosen to provide good rejection of events due to K^+ decay in flight. This is important because K^+ decays in flight in the mode $K^+ \rightarrow \pi^+ + \pi^0$, with the π^+ going slightly forward in the center of mass system, would have been a considerable background. The minimum time delay between a K^+ stop and the observation of a decay product was set at 6×10^{-9} seconds. To determine the rejection rate of prompt events that such a delay implies, the K^+ telescope was set to accept π^+ mesons. Charge exchange and scattering in S6 provided a convenient source of prompt events. The time distribution of these events is shown in Fig. 4. The rejection rate of

prompt events at the minimum delay time of 6×10^{-9} seconds was at least 200:1. This condition rendered negligible the background of K^+ decay in flight in the stopping counters. The delay time interval in which K^+ decays were accepted extended about 25×10^{-9} seconds beyond the minimum acceptable delay time.

In addition to the time delay condition set on the K^+ decay muon, pulse height criteria were applied to the T2, T3, and T4 scintillation counters. Since the energy loss of positrons in these counters was considerably less than the energy loss of the stopping muons, it was possible to reject positrons by using pulse height discrimination. In each of the counters, the minimum pulse height condition was set so that the efficiency for detecting positrons was rather low although the efficiency for detecting muons from $K^+ \rightarrow \mu^+ + \nu$ was greater than 95%. The efficiency for detecting stopping muons was therefore also greater than 95%. In addition to these lower limits on the pulse height, an upper limit was set on counter T2 so that events would not be detected in which a scattered K^+ meson stopped at an appreciable depth in T2 and decayed in a manner which simulated a decay originating from a K^+ stop in S6 or S6B. This condition had a negligible effect on the $K^+ \rightarrow \pi^0 + \mu^+ + \nu$ rate. Whenever the pulse height in the T4 counter was high enough to indicate that a muon had stopped in the counter, the information was displayed on the spark chamber photograph in the form of a marker lamp. Since muons stopping in plastic scintillator are depolarized[1], it was necessary to reject such events. This was done by rejecting all events in which the muon decay vertex appeared in the region of the T4 counter. The marker lamp information indicated that the rejection had been made correctly.

---

[1] R. Swanson, Phys. Rev. 112, 580(1958)

Because the T4 counter was only 1/16 in thick, the number of events rejected was not large.

It was necessary that the T5 anticoincidence counter be very efficient. For every muon that stopped between T4 and T5 from $K^+ \rightarrow \pi^o + \mu^+ + \nu$, about 250 muons from $K^+ \rightarrow \mu^+ + \nu$ passed through the stopping region and the anticoincidence counter. Any event not rejected by the anticoincidence counter would be identified as a forward $\mu \rightarrow e^+ + \nu + \bar{\nu}$ decay. In order to insure that the anticoincidence counter was efficient, it was DC coupled to the coincidence circuit. To determine that the counter was effective, we took a sample of photographs of the spark chambers in which the chambers normally revealing the muon decay were pulsed without the usual 3.3×10^{-6} second time delay. In this case the delay time was 0.34×10^{-6} second. The number of muon decays visible in the forward direction through the T5 counter decreased in accordance with the expectation based on the muon lifetime. A certain number of stopping muons decayed in the forward direction within 10^{-8} seconds after stopping. These were also rejected by the T5 counter. A small correction was made to the data to account for this loss. The loss of events caused by the T5 anticoincidence counter detecting the showers from the π^o decay gamma rays was computed by a Monte Carlo technique. The loss was less than 1% of the events.

Throughout the experiment, a scaler recorded the events occurring subject to the same conditions as the $K^+ \rightarrow \pi^o + \mu^+ + \nu$ events except that the T5 counter was in coincidence rather than anticoincidence. By scanning a sample of pictures which were taken with the spark chambers triggered by this scaler signal, it was established that 0.992 of these

events were caused by muons from $K^+ \rightarrow \mu^+ + \nu$.

The spark chambers were not all operated under the same conditions. The chambers numbered 1 to 6 in Fig. 3 were separated by 0.25 inch thick copper plates and were pulsed 340×10^{-9} seconds after the passage of a particle through the T2, T3, T4 counter telescope. There was a 40 volt clearing potential applied to these chambers to keep the resolving time short. The spark chambers numbered from 7 to 22 were operated with a 4 volt clearing potential and were pulsed 3.3×10^{-6} seconds after the passage of a particle through the counter telescope. Although the quality of the tracks in this section of spark chambers was not good because of the difference in ionization between the stopping muons and the decay positrons, and the difference in time between the passage of the particles, tracks were always visible. Frequently some of the sparks were, however, very weak. Both sets of spark chambers were filled with a 90% neon, 10% helium mixture, and were photographed with a lens opening of f 5.6 using Tri-X film.

The chance background rate in the spark chambers due to pions in the unseparated beam interacting in the K^+ degrader was such that there were frequently background tracks in the spark chambers in which the muon decays were observed. In these cases, the track in the short resolving time region of the spark chambers tagged the K^+ decay event. The number of events that were lost because background tracks overloaded the muon decay spark chambers was negligible.

In scanning the photographs, we accepted only those events in which the appearance of the particle track in the short resolving time region of the spark chambers was satisfactory, i.e. we required that there be no sparks missing in the track, and that there be no other sparks

within 1 cm. of the track. Furthermore, events which showed a single scatter of more than 20° were rejected. These conditions were used to reject positrons. The scanning loss of muon events was determined by applying the above conditions to a sample of muons from $K^{+} \rightarrow \mu^{+} + \nu$ which were known to be uncontaminated with positrons. The scanning efficiency measured with these events was 0.92 ± 0.01. A correction for this loss of muon events was made in the data analysis. In the sample of otherwise acceptable $K^{+} \rightarrow \pi^{0} + \mu^{+} + \nu$ events, 12% of the events violated one of the above scanning conditions. Since we expected a loss of 8% because of the spark chamber inefficiency as measured with the $K^{+} \rightarrow \mu^{+} + \nu$ events, we assumed that the remaining 4% are positrons which did not violate the pulse height conditions set on the counters. This assumption is supported by the observation that the rejected events did not show as many decay vertices as would have been expected from muon decays.

C. Muon Range Determination Procedure

The energy of a stopping muon was determined from its range. In the range measurement we took into account the depth in the S6, S6B stopping region at which the K^{+} decay took place, and the angle of incidence of the muon on the spark chamber plates. The analysis procedure is as follows. The range of the muon was assigned a bin number equal to the number of the last spark chamber in which the muon was visible. If the S6B marker lamp indicated that the K^{+} had stopped in S6B, the bin number was increased by one in order to account for the energy loss of

the muon in crossing counter S6. The counter thickness was chosen to be equivalent to one spark chamber plate. The angle between the normal to the spark chamber plates and the path of the muon as it crossed the first two spark chambers after leaving the K^+ stopper was measured in each event. If this angle was between 14.5° and 20.5° the bin number was increased by one. If the angle was between 20.5° and 24.5° the bin number was increased by two. Events with a total correction of more than two bins were rejected.

To determine the average initial kinetic energy corresponding to the various bins after making the corrections described above, a small amount of degrader was removed from the spark chambers in order that pions from the decay $K^+ \rightarrow \pi^+ + \pi^0$ would stop in the carbon plate region. The bin distribution of these events is shown in Fig. 5. The range energy tables of Sternheimer[2] were used to derive from this observed pion range the energy of a muon with the same range, and to account for the small amount of additional degrader used in the muon experiment. A similar procedure was applied to compute the bin energy from the distribution of stopping muons from $K^+ \rightarrow \mu^+ + \nu$. The energy scales computed by these two different procedures differed by 1.7 MeV. An average of the two has been chosen. An absolute error in energy scale of one bin or ± 2.75 MeV has been assumed in the data analysis. The energy resolution function shown in Fig. 5 caused a negligible distortion of the muon spectrum in $K^+ \rightarrow \pi^0 + \mu^+ + \nu$.

---

[2] D. Ritson, Techniques of High Energy Physics, Appendix V by R. M. Sternheimer, Interscience, New York 1961.

DATA ANALYSIS

A. Decay Rate Measurement

The efficiency for detecting particles was a function of the range. This variation in efficiency was caused by two factors: (1) The varying angle of incidence of the muons on the spark chamber plates, and (2) the varying depth in the K^+ stopping counters at which the muons originated. The first range interval in which the muons could stop and be detected (No. 11) contained only those events in which the K^+ stopped in S6 and the deviation of the muon from normal incidence on the spark chamber plates was less than 14.5°. On the other hand, in range interval No. 15, the events could come from K^+ stops in S6 or S6B, and from a variety of incidence angles. Since the scaler counting muons from $K^+ \rightarrow \mu^+ + \nu$ was sensitive to all K^+ decays because the T5 counter was much larger than the solid angle subtended by the T3, T3, T4 telescope, it was necessary to determine the efficiency for detecting stopping muons. To determine the efficiency S(j) for detecting particles stopping in range interval j after the various corrections, additional degrader was added to the spark chambers in order that muons from $K^+ \rightarrow \mu^+ + \nu$ stopped in the center of the carbon plate region. The number of events in each range correction category was measured. The value of S(11) for example was equal to the total number of events in which the K^+ decay occurred in S6 and in which the muon deviated from normal incidence on the spark chambers by less than 14.5° divided by the total number of $K^+ \rightarrow \mu^+ + \nu$ events observed. In Table I, S(j) has been divided by 0.964. This constant factor has been combined with other correction factors such as the

spark chamber scanning efficiency.

We calculated the background from the decay in flight of π^+ mesons from $K^+ \rightarrow \pi^o + \pi^+$ in the following manner. We followed a number of pions equal to $\frac{\Gamma(K^+ \rightarrow \pi^o + \pi^+)}{\Gamma(K^+ \rightarrow \mu^+ + \nu)}$ times the number of scaler counted $K^+ \rightarrow \mu^+ + \nu$ events until they stopped in the degrader region of the spark chamber assembly. We assumed that the attenuation coefficient by nuclear interactions in copper is 1/105 cm^2/gram. Since the change in the laboratory trajectory of the charged particle in those $\pi^+ \rightarrow \mu^+ + \nu$ decays in which the muon reached the carbon plates in the stopping region was too small to be observed, the background consisted of all such decays. The total rate of decay per centimeter of path length is $\frac{1}{\beta\gamma c\tau}$ where τ is the pion mean life (25.5×10^{-9} seconds). The average component of the polarization in the direction of the pion line of flight of the muons coming to rest at a particular range in the carbon plates is equal to $-\cos\theta$ where θ is the angle in the center of mass system between the line of flight of the pion and the direction of the muon. The events from pion decay in flight are assumed to be subject to the same scanning losses and corrections as the $K^+ \rightarrow \pi^o + \mu^+ + \nu$ events. There is considerable disagreement among the various experimental determinations of the ratio of the $K^+ \rightarrow \pi^o + \pi^+$ decay rate to the $K^+ \rightarrow \mu^+ + \nu$ decay rate that have been published. In making the above calculation, the value of $\frac{\Gamma(K^+ \rightarrow \pi^o + \pi^+)}{\Gamma(K^+ \rightarrow \mu^+ + \nu)}$ has been assumed to be 0.37 ± 0.06. The assumed error is wide enough to overlap most of the experimental results.*

---

*This situation has been clarified in the recently published work of F. Shaklee, C. Jensen, B. Roe, and D. Sinclair, Phys. Rev. 136, B1423 (1964). These authors find the best value for the $K^+ \rightarrow \pi^o + \pi^+ / K^+ \rightarrow \mu^+ + \nu$ decay rate ratio to be 0.356 ± 0.015.

We have calculated the background from the radiative decay $K^+ \rightarrow \mu^+ + \nu + \gamma$ from the matrix element derived by Cabibbo.[3] This matrix element, in which the so called structure dependent effects have been neglected, is:

$$M = -\frac{G}{\sqrt{2}} M_K f_a \sqrt{4\pi}\, e \frac{M_\mu}{2p_\mu \cdot k} \bar{U}_\mu (\not{\epsilon}\not{k} + 2p_\mu \cdot \epsilon)(1+\gamma_5) U_{\nu,\mu} \tag{4}$$

M_K and M_μ are the K and μ masses, p_μ is the muon four momentum, and ϵ, k are the photon polarization and four momentum. The form factor f_a is defined by M_o, the matrix element for $K^+ \rightarrow \mu^+ + \nu$:

$$M_o = -\frac{iG}{\sqrt{2}} M_K f_a \bar{U}_\mu \not{p}_\mu (1+\gamma_5) U_{\nu,\mu} \tag{5}$$

We computed from these matrix elements the energy distribution and the longitudinal polarization of the muons. We assumed that the γ ray has not been detected. The results are as follows.

Muon Polarization:

$$P = -B(E_\mu)/A(E_\mu) \tag{6a}$$

Muon Energy Distribution:

$$\frac{d\Gamma(K^+ \rightarrow \mu^+ + \nu + \gamma)}{dE_\mu} = \Gamma_o A(E_\mu) \frac{e^2}{2\pi P_{max}^2} \tag{6b}$$

In the above expression, Γ_o is approximately equal to the observed rate of

---

[3] N. Cabibbo, Nuovo Cimento 11, 827(1959)

$K^+ \rightarrow \mu^+ + \nu$. The two functions $A(E_\mu)$ and $B(E_\mu)$ are:

$$A(E_\mu) = (E_{max}-E_\mu)\log f + \frac{4E_\mu P_{max}}{E_{max}-E_\mu}\left(\log g - \frac{P_\mu}{E_\mu}\right) \tag{7}$$

$$B(E_\mu) = \frac{(E_{max}-E_\mu)(M_K E_\mu - M_\mu^2)\log f}{M_K P_\mu} + \frac{4E_\mu(E_{max}E_\mu - M_\mu^2)\log g}{P_\mu(E_{max}-E_\mu)} - \frac{2(E_{max}^2 + E_\mu^2 - 2M_\mu^2)}{(E_{max}-E_\mu)} \tag{8}$$

The functions f and g in the above equations are defined as follows:

$$f = \frac{M_k(E_\mu + P_\mu) - M_\mu^2}{M_k(E_\mu - P_\mu) - M_\mu^2}$$

$$g = \frac{E_\mu + P_\mu}{M_\mu}$$

$$P_{max} = \frac{M_k^2 - M_\mu^2}{2\,M_k}$$

$$E_{max} = \frac{M_k^2 + M_\mu^2}{2\,M_k}$$

In these expressions E_μ and P_μ are the total energy and momentum of the muon. The units have been chosen such that $e^2 = 1/137$ and $c = 1$. The results of the above calculation are shown in Figs. 6 and 7.

The background from the decay in flight of muons from $K^+ \rightarrow \mu^+ + \nu$ was computed taking into account the muon lifetime, the effect of the T5 anticoincidence counter, and the annihilation in flight of the decay positrons.

The observed rate for $K^+ \rightarrow \pi^o + \mu^+ + \nu$ after the above described backgrounds have been subtracted is given in the last column of Table I. In order to make comparisons with various theoretical predictions, it is of interest to determine the rate relative to the total rate for the process $K^+ \rightarrow \pi^o + e^+ + \nu$. The total number of these events corresponding to the data of Table I has been obtained by multiplying the observed number of $K^+ \rightarrow \mu^+ + \nu$ events by the factor $\frac{\Gamma(K^+ \rightarrow e^+ + \pi^o + \nu)}{\Gamma(K^+ \rightarrow \mu^+ + \nu)}$ which has been obtained from a number of experiments.[4] This factor is taken to be 0.076 ± .007. The results of the rate measurement may be summarized by the following expression:

$$\frac{\int_{107.1}^{126.4} \frac{d\Gamma(K^+ \rightarrow \pi^o + \mu^+ + \nu)}{dE_\mu} S(E_\mu)\, dE_\mu}{\Gamma(K^+ \rightarrow \pi^o + e^+ + \nu)} = 0.0445 \pm 0.007$$

The error takes into account the statistical uncertainties, and the error in determining the muon energy scale. The $S(E_\mu)$ factor is the same as that given in Table I. If the data are corrected for the efficiency function, the results may be expressed as follows:

---

[4] Rosenfeld, Barbaro-Galtieri, Barkas, Bastien, and Kirz, Rev. Mod. Phys. 36, 977 (1964)

$$\frac{\int_{107.1}^{126.4} \frac{d\Gamma(K^+ \to \pi^0 + \mu^+ + \nu)}{dE_\mu} dE_\mu}{\Gamma(K^+ \to \pi^0 + e^+ + \nu)} = 0.054 \pm 0.008$$

The above expression has not been used in the data analysis.

B. Muon Longitudinal Polarization Measurement

We measured the polarization of the muons by observing the spatial asymmetry of the decay positrons. The angular distribution of positrons from the decay of polarized muons is:

$$W(\theta) = \frac{1}{2}\left(1 + \frac{P}{3}\cos\theta\right) \tag{9}$$

θ is the angle between the muon polarization P and the direction of the decay positron. This formula is correct only if the decay positrons are detected with an efficiency which does not depend on their energy. Since the apparatus used in this experiment was fully sensitive to positrons with an energy greater than 10 MeV, the correction due to the detection efficiency of the apparatus is negligible. In the analysis described here, θ was taken as the angle between the direction of the muon incident on the copper degrader and the direction of the decay positron. This choice reduced the effect of multiple scattering of the muon in the degrader. The multiple scattering of the muon (15° average) was such that even if the spin remained parallel to the momentum, the apparent attenuation of the polarization would be negligible. Likewise, the uncertainty (15° average) in the measurement of the decay positron

direction had a negligible effect.

The presence of magnetic fields as small as a few gauss appreciably modifies the angular distribution of positrons from the decay of polarized muons. In order to reduce the effect of the stray magnetic field of the Bevatron, the apparatus was placed so that the direction of motion of the muons was parallel to the stray field. At the peak of the magnet current cycle when the Bevatron beam spill occurred, the total magnetic field including that of the Earth was less than three gauss, and was within 30° of being parallel to the direction of motion of the muons. The sample of muon decays we used included those from the time of stopping to 3.3×10^{-6} seconds thereafter. The reduction of the longitudinal polarization of such a sample under our conditions is less than 2%.

We tested the performance of the apparatus as a polarization analyzer using muons from $K^{+} \rightarrow \mu^{+} + \nu$ which were brought to rest in the carbon plates. In Fig. 8a we show the observed angular distribution of the decay positrons. The solid line is a plot of the distribution expected for 100% negative polarization, i.e. $W(\theta) = \frac{N}{2}(1 - \frac{1}{3}\cos\theta)$ where N is the total number of events in the sample. In this sample, the minimum signature of a positron from muon decay was a single spark. The $K^{+} \rightarrow \pi^{0} + \mu^{+} + \nu$ experiment was carried out under conditions of a somewhat higher beam rate and occassionaly a single, unrelated spark would have been spuriously identified as a positron from a muon decay. In order to eliminate this possibility a minimum of three sparks along the positron track was required. The distribution of the $K^{+} \rightarrow \mu^{+} + \nu$ events with the three spark requirement is shown in Fig. 8b. Evidently the efficiency for detecting muon decays with the positron moving parallel

to the spark chamber plates was greatly reduced by this condition. Therefore, in making the polarization analysis, only those events with $\theta < 60^\circ$ and $\theta > 120^\circ$ were used. The three spark condition had only a small effect on the efficiency for observing these events. The polarization computed from these events did not depend on the value chosen for the cut-off angle.

We determined the polarization by a maximum likelihood analysis. The likelihood,

$$L \propto \prod_j (1 + \frac{P}{3} \cos\theta_j) \tag{10}$$

has been computed as a function of the assumed polarization P. In this expression θ_j is the angle between the direction of the positron and the direction of the incident muon for each event. We accepted for analysis only those events with $\theta_j < 60^\circ$ or $\theta_j > 120^\circ$. Fig. 9 shows the likelihood L for the polarization of the $K^+ \rightarrow \mu^+ + \nu$ events. The distribution has a mean of -0.94 and a standard deviation of 0.21. This result is consistent with the result of Coombes et al,[5] who found $P = -0.93 \pm 0.12$. A muon polarization of -1.0 is expected if the K^+ has zero spin and the neutrino is emitted in a state of complete negative longitudinal polarization.

The angular distribution of the muon decay positrons in the $K^+ \rightarrow \pi^0 + \mu^+ + \nu$ and background events is shown in Fig. 8c. The maximum likelihood analysis of this data is shown in Fig. 10. The observed polarization is 0.0 with a standard deviation of 0.22. The observed polarization

---

[5] Coombes, Cork, Galbraith, Lambertson, and Wenzel, Phys. Rev. 108, 1348(1957)

must be corrected to account for the large background which is negatively polarized. In the total of 864 events, there was a calculated contamination of 195.6 π^+ decay in flight events, with an average polarization of -0.69. There were 174.9 $K^+ \rightarrow \mu^+ + \nu + \gamma$ events with an average polarization of -0.98, and 4.3 μ^+ decay in flight events with an average simulated polarization of 0.0. In order to account for the fact that the T5 anticoincidence counter rejected forward muon decays within 10^{-8} seconds after the muon came to rest, a single event in the forward direction has been added to the above sample. After these corrections, the polarization of the muons from $K^+ \rightarrow \pi^+ + \mu^+ + \nu$ was determined to be $+0.61 \pm 0.39$, i.e.:

$$\frac{\int_{107.1}^{126.4} \frac{d\Gamma(K^+ \rightarrow \pi^o + \mu^+ + \nu)}{dE_\mu} S(E_\mu) P_\mu dE_\mu}{\int_{107.1}^{126.4} \frac{d\Gamma(K^+ \rightarrow \pi^o + \mu^+ + \nu)}{dE_\mu} S(E_\mu) dE_\mu} = +0.61 \pm 0.39$$

DISCUSSION OF RESULTS

In order to interpret these results, a number of assumptions are necessary. We shall assume that the neutrino emitted in the $K^+ \rightarrow \pi^o + \mu^+ + \nu$ decay is in a state of complete negative longitudinal polarization. The most general local, Lorentz invariant matrix element not involving derivatives of the fields can be than written as follows:[6, 7, 8, 9, 10]

$$M = \frac{G}{\sqrt{2}} (\bar{U}_\mu [M_K f_s + i(f_+(P+Q) + f_-(P-Q))\cdot\gamma + \frac{if_t}{2M_K}(P_a Q_b - P_b Q_a)\sigma_{ab}](1+\gamma_5)U_{\nu,\mu}) \tag{11}$$

In this expression, P is the four momentum of the K^+ meson, and Q is the four momentum of the π^o meson. Each of the form factors (i.e. f_s, f_+, f_-, and f_t) may be functions of the square of the four momentum transfer to the muon-neutrino pair, $s = (P-Q)^2$. It will be convenient for the following discussion to make the definition $\xi(s) = \frac{f_-(s)}{f_+(s)}$ for the vector form

[6] J. D. Jackson, ELEMENTARY PARTICLES AND FIELD THEORY, 1962 BRANDEIS LECTURES, Vol. 1, Benjamin, New York 1963

[7] J. Werle, Nuclear Physics 6, 1 (1958)

[8] P. Dennery and H. Primakoff, Phys. Rev. 131, 1334 (1963)

[9] N. Brene, L. Egardt, and B. Qvist, Nuclear Physics 22, 553 (1961)

[10] L. Okun, Nuclear Physics 5, 455 (1958)

factor ratio.

The term in the matrix element proportional to f_- can be recast in the form of a scalar interaction with an effective coupling constant equal to $-M_\mu f_-$. For this reason, there are actually only three independent quantities to be determined. The true scalar interaction differs, however, from the scalar interaction generated by the f_- term in the vector interaction in that the factor M_ℓ (ℓ = lepton) is not present. These two scalar terms thus behave differently under the interchange of muon and electron. In the $K^+ \rightarrow \pi^o + e^+ + \nu$ decay, the contribution of a f_- term is much smaller than in the $K^+ \rightarrow \pi^o + \mu^+ + \nu$ decay. It is therefore possible in principle to separate the two types of scalar interaction by comparing the two different decay modes given above.

In the present experiment, the π^o was not observed. In order to make predictions using the matrix element M it is therefore necessary to know the momentum transfer dependence of the form factors. For the remainder of this discussion, we shall assume that they are independent of momentum transfer. Arguments based on a dispersion relation treatment of the form factors indicate that they vary only a small amount over the region of momentum transfer possible in the $K^+ \rightarrow \pi^o + \mu^+ + \nu$ decay.[11]

We have computed the longitudinal polarization of the muons as a function of muon energy for pure scalar, vector ($\xi = 0$), and tensor couplings. The results are shown in Fig. 11. The polarization we observe is not consistent with a pure scalar or a pure tensor coupling.

---

[11] J. Bernstein and S. Weinberg, Phys. Rev. Letters 5, 481 (1960)

Furthermore, additional calculations[†] have shown that there is only one combination of scalar and tensor coupling that has a polarization consistent with the experimental result. This combination ($f_t/f_s = 5$, $\delta\theta_{st} = 180^\circ$), however, requires a negative polarization of the muons below a kinetic energy of 95 MeV. There have been two recent experiments[12, 13] in which the muon polarization was observed at kinetic energies in the 70 MeV region. In each experiment the observed polarization was positive. For this reason it is possible to exclude the scalar tensor mixture as a possible solution. It is therefore necessary that the vector interaction be at least partly responsible for the decay $K^+ \rightarrow \pi^0 + \mu^+ + \nu$.

For the remainder of the discussion we shall assume that the interaction is of a pure vector type and that the form factors are constant. Assuming this, the matrix element for the decay is:

$$M = C_\mu [\, \bar{U}_\mu ((P+Q) + \xi(P-Q)) \cdot \gamma(1+\gamma_5) U_{\nu,\mu}] \qquad (12)$$

In the above expression C_μ is a constant. The above matrix element leads

---

[†] We have used the expression derived by Okun[10] for this analysis after making the following changes: (1) We assume the expression applies to K^+ decay rather than K^- decay, (2) $\bar{A}$, $\bar{B}$, $\bar{C}$, and $\bar{D}$ are replaced by $\bar{A}/M_K^2$, $\bar{B}/M_K^2$, $\bar{C}/M_K$, and $\bar{D}/M_K$, and (3) the interference terms f_{sv}, f_{st}, and f_{vt} have been multiplied by 2.

[12] V. Smirnitski and A. Weissenberg, Phys. Rev. Letters 12, 233 (1964)

[13] Gidal, Powell, March, and Natali, Phys. Rev. Letters 13, 95 (1964)

to a component of muon polarization out of the plane of the decay proportional to the imaginary part of ξ. Hence, the assumption of time reversal invariance would require that ξ be real. Recent experimental results on K_2^o decay have indicated that time reversal invariance may be violated.[14] For this reason, we shall not assume ξ is real in the present discussion.

For comparison with the experimental polarization measurement, the following function has been computed from the above matrix element:

$$P(E_\mu)_{av} = \frac{\int_{107.1}^{126.4} \frac{d\Gamma(K^+ \to \pi^o + \mu^+ + \nu)}{dE_\mu} S(E_\mu)P(E_\mu)\, dE_\mu}{\int_{107.1}^{126.4} \frac{d\Gamma(K^+ \to \pi^o + \mu^+ + \nu)}{dE_\mu} S(E_\mu)\, dE_\mu} \qquad (13)$$

In the above expression, $S(E_\mu)$ is the energy dependent detection efficiency given in Table I, and $P(E_\mu)$ is the muon longitudinal polarization. The above expression depends only on ξ being independent of the constant factor C_μ. The result of this calculation is shown in Fig. 12. If ξ is real, the experimental result requires that $-4.0 < \xi < +1.7$. We have used the expressions derived by Dennery and Primakoff[8] and by Brene, Egardt, and Qvist[9] in the above analysis.

In order to calculate the absolute rate of $K^+ \to \pi^o + \mu^+ + \nu$ decay, it is necessary to know the value of the constant C_μ as well as the value of ξ. By making the assumption that the weak coupling strength

[14] Christenson, Cronin, Fitch, and Turlay, Phys. Rev. Letters 13, 138 (1964)

of muons is the same as that of electrons, it is possible to determine C_μ from the observed rate of $K^+ \to \pi^o + e^+ + \nu$ decay. This assumption is equivalent to the statement that the matrix element used for the computation of the $K^+ \to \pi^o + e^+ + \nu$ decay is the same as that used for the computation of the $K^+ \to \pi^o + \mu^+ + \nu$ decay except that m_e is substituted for m_μ wherever the lepton mass appears. Making this assumption, we have computed the ratio of the rate at which muons from $K^+ \to \pi^o + \mu^+ + \nu$ stopped in our apparatus to the total rate of $K^+ \to \pi^o + e^+ + \nu$ decay.

$$\text{Rate} = \frac{\displaystyle\int_{107.1}^{126.4} \frac{d\Gamma(K^+ \to \pi^o + \mu^+ + \nu)}{dE_\mu} S(E_\mu)\, dE_\mu}{\displaystyle\int_0^{E_{max}} \frac{d\Gamma(K^+ \to \pi^o + e^+ + \nu)}{dE_e}\, dE_e} \tag{14}$$

This function depends only on ξ. The result of this calculation is shown in Fig. 12. If ξ is real, the observed decay rate implies that $+0.2 < \xi < +1.4$ or $-4.8 < \xi < -3.5$.

In Fig. 12 we have combined the results and the theoretical predictions for the muon polarization and decay rate. The solution with $+0.2 < \xi < +1.4$ is evidently the most probable provided that ξ is real. Solutions with ξ imaginary, as suggested by Cabibbo[15], are also possible. In that case, the results imply that $0.8 < |\xi| < 2.6$. It is important to note that the experimental point in Fig. 12 is consistent with at least one value of ξ. If the muon weak coupling strength C_μ were

[15] N. Cabibbo, Physics Letters 12, 137 (1964)

appreciably different from the electron weak coupling strength C_e, the experimental result would not be consistent with any value of ξ. In order that the experimental result be consistent with at least one value of ξ, it is necessary that $0.77 < \frac{|C_\mu|}{|C_e|} < 1.48$.

The ratio of the differential muon spectrum in $K^+ \rightarrow \pi^o + \mu^+ + \nu$ to the total rate of $K^+ \rightarrow \pi^o + e^+ + \nu$ has been computed for $\xi = +0.84$. The computation and the experimental results corrected for the detection efficiency are shown in Fig. 13.

The $K^+ \rightarrow \pi^o + \mu^+ + \nu$ decay has been investigated in a number of experiments. The results of the present experiment are consistent with the results of the experiments of Gidal et al.,[13] Smirnitski and Weissenberg,[12] Jensen et al.,[16] and Brown et al.[17] Our results are not in agreement with various aspects of the experiments of Dobbs et al.,[18] and Boyarski et al.[19]

---

[16] Jensen, Shaklee, Roe, and Sinclair, Phys. Rev. 136, B1430 (1964)

[17] Brown, Kadyk, Trilling, and Van de Walle, Phys. Rev. Letters 8, 450 (1962)

[18] Dobbs, Lande, Mann, Reibel, Sciulli, Uto, White, and Young, Phys. Rev. Letters 8, 295 (1962)

[19] Boyarski, Loh, Niemela, Ritson, Weinstein, and Ozaki, Phys. Rev. 128, 2398 (1962)

SUMMARY

An analysis assuming a pure vector interaction with constant form factors and equal muon and electron weak coupling strength has been shown to be consistent with the experimental observations. The vector form factor ratio ξ can be real or imaginary. The probable solutions for ξ are shown in Fig. 12. There is no evidence on the basis of the present experiment that the form of the leptonic weak interaction current J_λ^ℓ in the coupling to the current of the strongly interacting particles which changes strangeness J_λ^s, $\Delta s = 1$ is different from the form of J_λ^ℓ in the coupling to the currents which do not change strangeness.

ACKNOWLEDGEMENTS

We wish to thank Prof. E. Segrè for his advice and encouragement, and Drs. N. Cabibbo and W. Chinowsky for many helpful discussions. Many of the calculations were made by Mr. A. Maksymowicz. The Bevatron operation was under the supervision of W. Hartsough.

TABLE I

Range Bin	Average Energy	Events	S	Calculated Backgrounds: $K^+ \to \mu^+ + \nu + \gamma$ Events	$K^+ \to \mu^+ + \nu + \gamma$ Polarization	$K^+ \to \pi^0 + \pi^+$ d.i.f. Events	$K^+ \to \pi^0 + \pi^+$ d.i.f. Polarization	$K^+ \to \mu^+ + \nu$ d.i.f. Events	(Events) — (Background)
1	108.5	114	0.484	9.5	-0.97	22.6	-0.56	0.6	81.3
2	111.25	108	0.888	19.0	-0.97	34.2	-0.59	0.5	54.3
3	114.0	164	1.000	23.5	-0.98	33.0	-0.64	0.7	106.8
4	116.75	142	1.000	25.9	-0.98	29.7	-0.68	0.7	85.7
5	119.5	128	1.000	28.7	-0.98	29.6	-0.76	0.6	69.1
6	122.25	108	1.000	32.1	-0.99	24.8	-0.80	0.6	50.5
7	125.0	100	1.000	36.2	-0.99	21.7	-0.86	0.6	41.5
8	127.75	70	1.000	41.2	-0.99	17.2	-0.89	0.4	11.2
9	130.5	33	0.498	24.5	-0.99	7.5	-0.95	0.2	0.8

Number of $K^+ \to \mu^+ + \nu$ events = 166,169

Stopping muon detection efficiency other than S(j) = 0.876

d.i.f. = decay in flight

FIGURE CAPTIONS

1. Magnet system of 470 MeV/c unseparated K^+ beam.

2. Stopping K^+ rate as function of second bending magnet current.

3. Side view of spark chamber assembly. The unseparated beam passes through the counter telescope at the top of the assembly. K^+ mesons stop in the counters numbered S6 and S6B.

4. Time distribution of prompt coincidences between beam telescope and muon telescope with beam telescope set to accept pions and positrons. Additional degrader has been added in the beam telescope to stop K mesons before S6.

5. Range distribution of π^+ mesons from $K^+ \rightarrow \pi^o + \pi^+$. Part of the degrader in the spark chamber assembly has been removed to permit this measurement.

6. Energy distribution of μ^+ in the decay $K^+ \rightarrow \mu^+ + \nu + \gamma$. It is assumed that the gamma ray is not detected.

7. Longitudinal polarization of μ^+ in the decay $K^+ \rightarrow \mu^+ + \nu + \gamma$. It is assumed that the gamma ray is not detected.

8. Angular distribution of positrons from μ^+ decay. (a) Muons from $K^+ \rightarrow \mu^+ + \nu$ with a minimum positron signature of 1 spark. (b) Muons from $K^+ \rightarrow \mu^+ + \nu$ with a minimum positron signature of 3 sparks. (c) Muons from background events and $K^+ \rightarrow \pi^o + \mu^+ + \nu$ with a minimum positron signature of 3 sparks.

9. Likelihood plot for longitudinal polarization of muons in $K^+ \rightarrow \mu^+ + \nu$.

10. Likelihood plot for longitudinal polarization of muons in $K^+ \rightarrow \pi^0 + \mu^+ + \nu$ and background events.

11. Longitudinal polarization of muons in $K^+ \rightarrow \pi^0 + \mu^+ + \nu$ for pure scalar, vector ($\xi = 0$), and tensor couplings. The polarization for vector coupling with $\xi = \infty$ is identical to that for scalar coupling. The experimental point is not consistent with pure scalar or tensor coupling.

12. Muon longitudinal polarization and energy spectrum assuming pure vector coupling, constant form factors, and equal muon and electron coupling strengths. The curve is the locus of points with varying vector form factor ratio ξ .

13. Energy distribution of muon in $K^+ \rightarrow \pi^0 + \mu^+ + \nu$. The experimental points have been corrected to account for backgrounds and the varying detection efficiency.

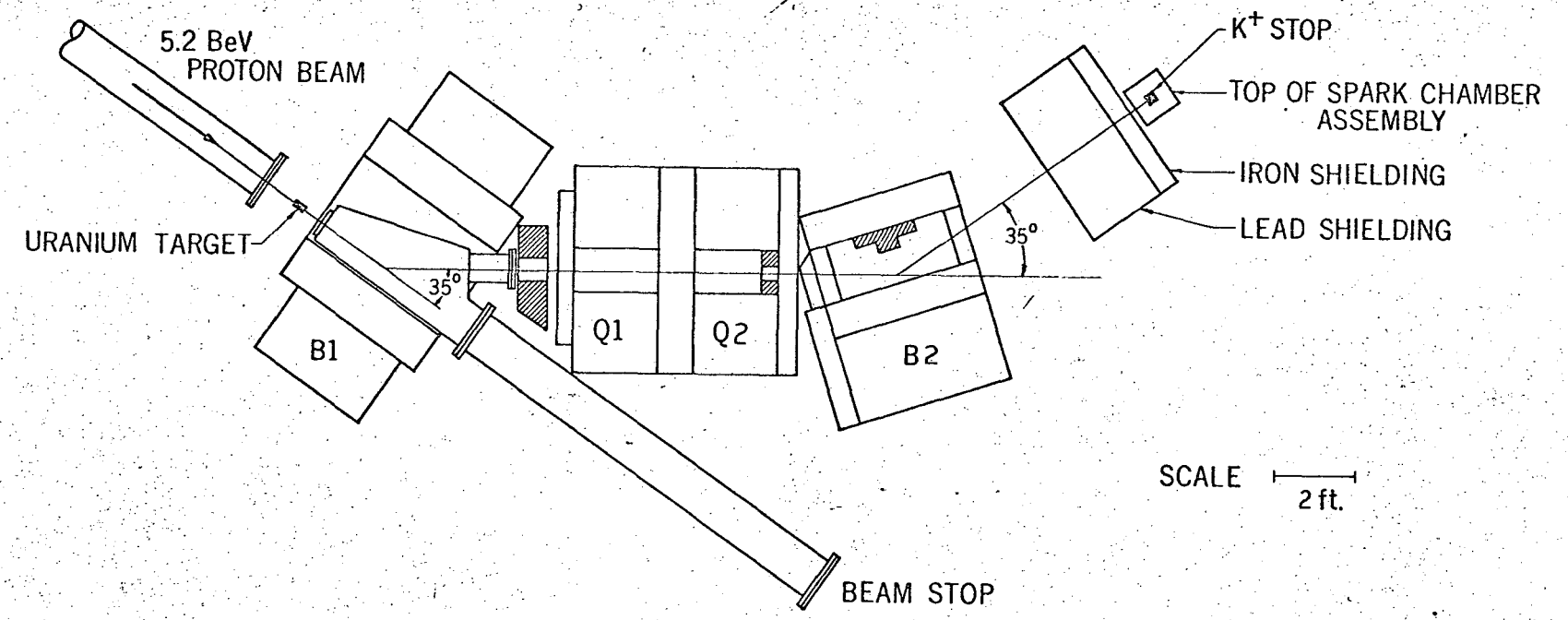
5.2 BeV
PROTON BEAM
URANIUM TARGET
35°
B1
Q1
Q2
B2
35°
K+ STOP
TOP OF SPARK CHAMBER
ASSEMBLY
IRON SHIELDING
LEAD SHIELDING
SCALE
2 ft.
BEAM STOP

Fig. 1

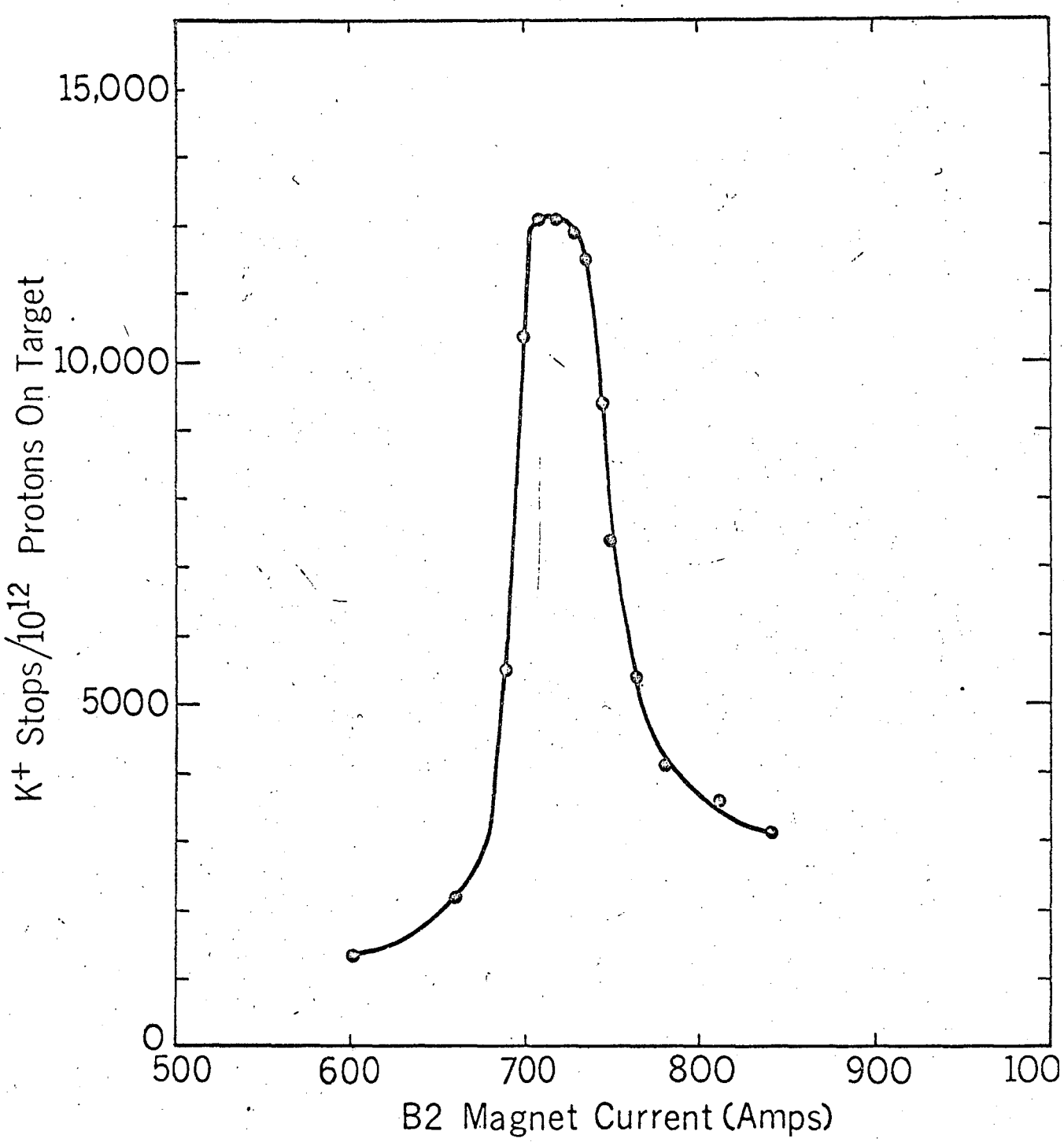
15,000
10,000
5000
0
K+ Stops/10^12 Protons On Target
500
600
700
800
900
100
B2 Magnet Current (Amps)

Fig. 2

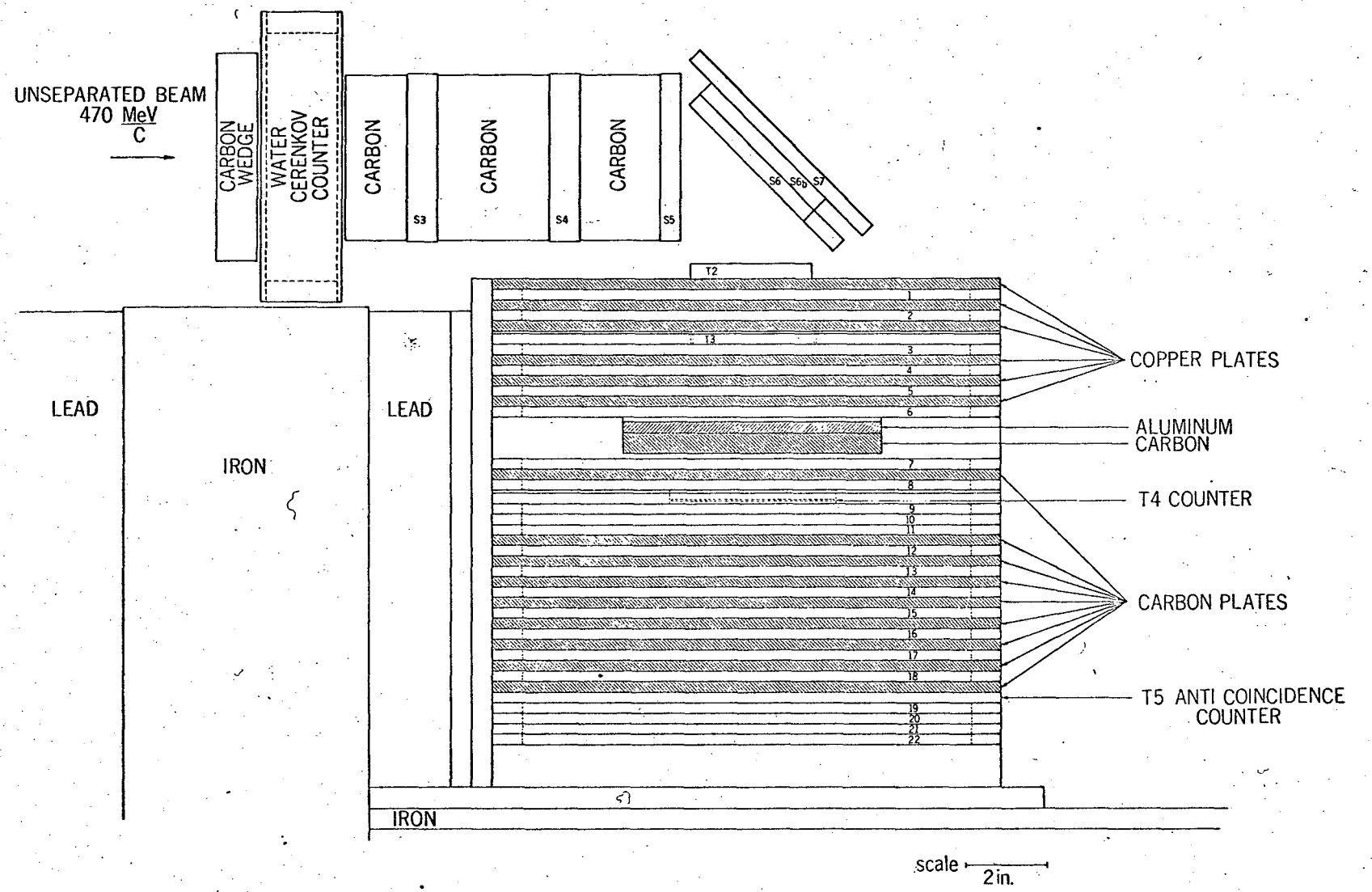
UNSEPARATED BEAM
470 MeV/C
CARBON WEDGE
WATER CERENKOV COUNTER
CARBON
S3
CARBON
S4
CARBON
S5
S6
S6b
S7
T2
T3
LEAD
IRON
LEAD
IRON
COPPER PLATES
ALUMINUM
CARBON
T4 COUNTER
CARBON PLATES
T5 ANTI COINCIDENCE COUNTER
scale
2 in.

Fig. 3

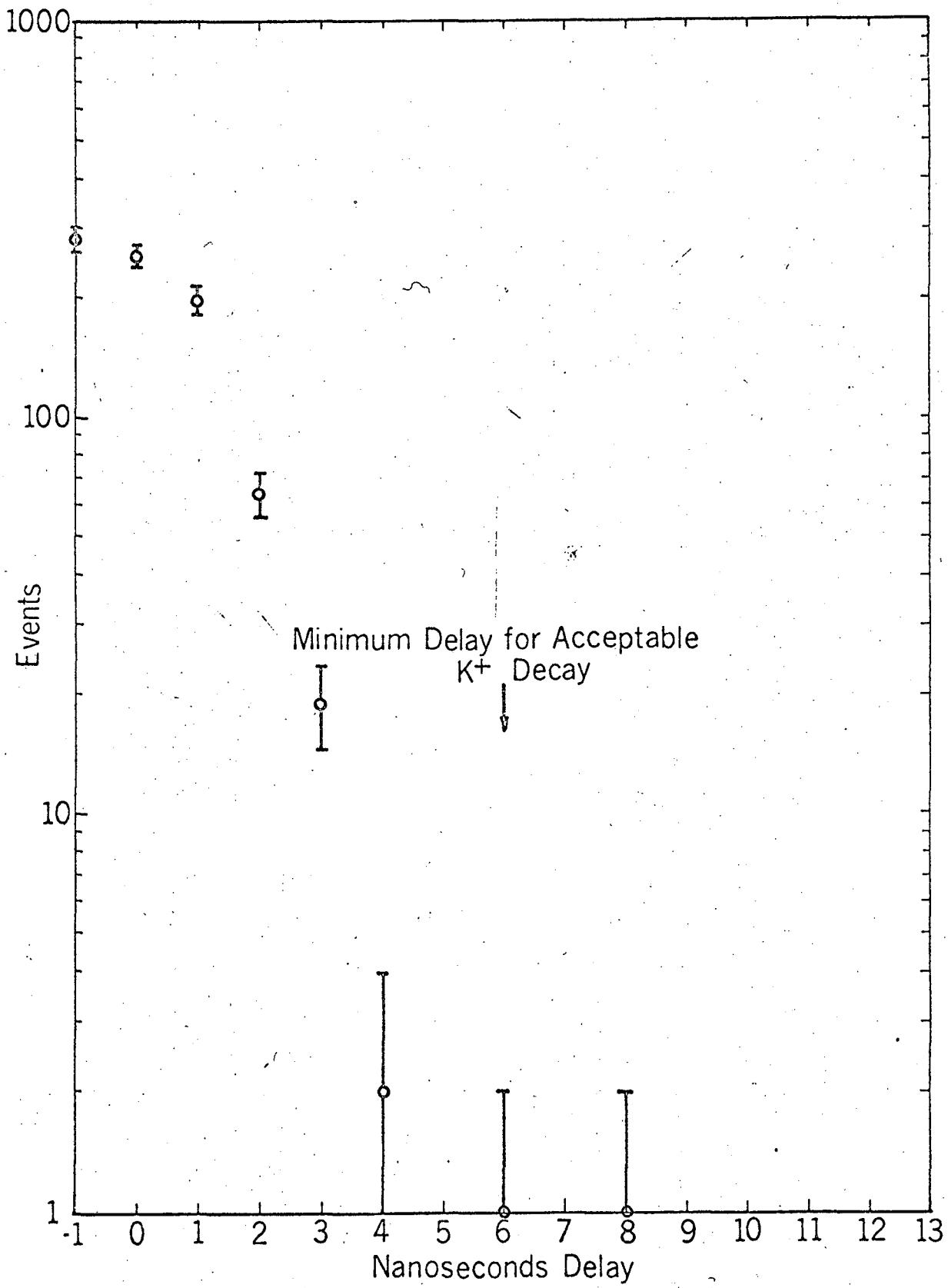
1000
100
10
1
Events
Minimum Delay for Acceptable
K+ Decay
-1
0
1
2
3
4
5
6
7
8
9
10
11
12
13
Nanoseconds Delay

Fig. 4

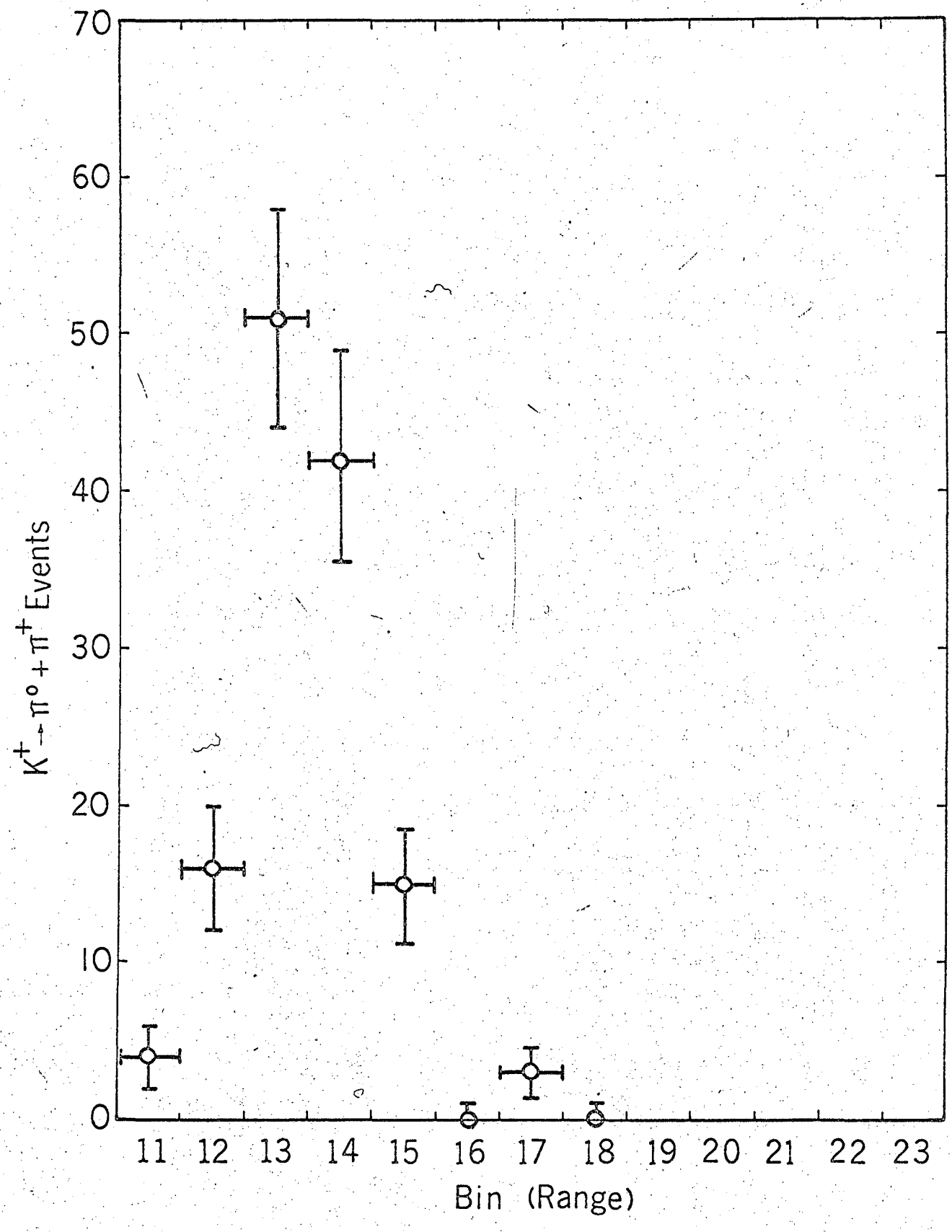
70
60
50
40
30
20
10
0
$K^+ \to \pi^0 + \pi^+$ Events
11 12 13 14 15 16 17 18 19 20 21 22 23
Bin (Range)

Fig. 5

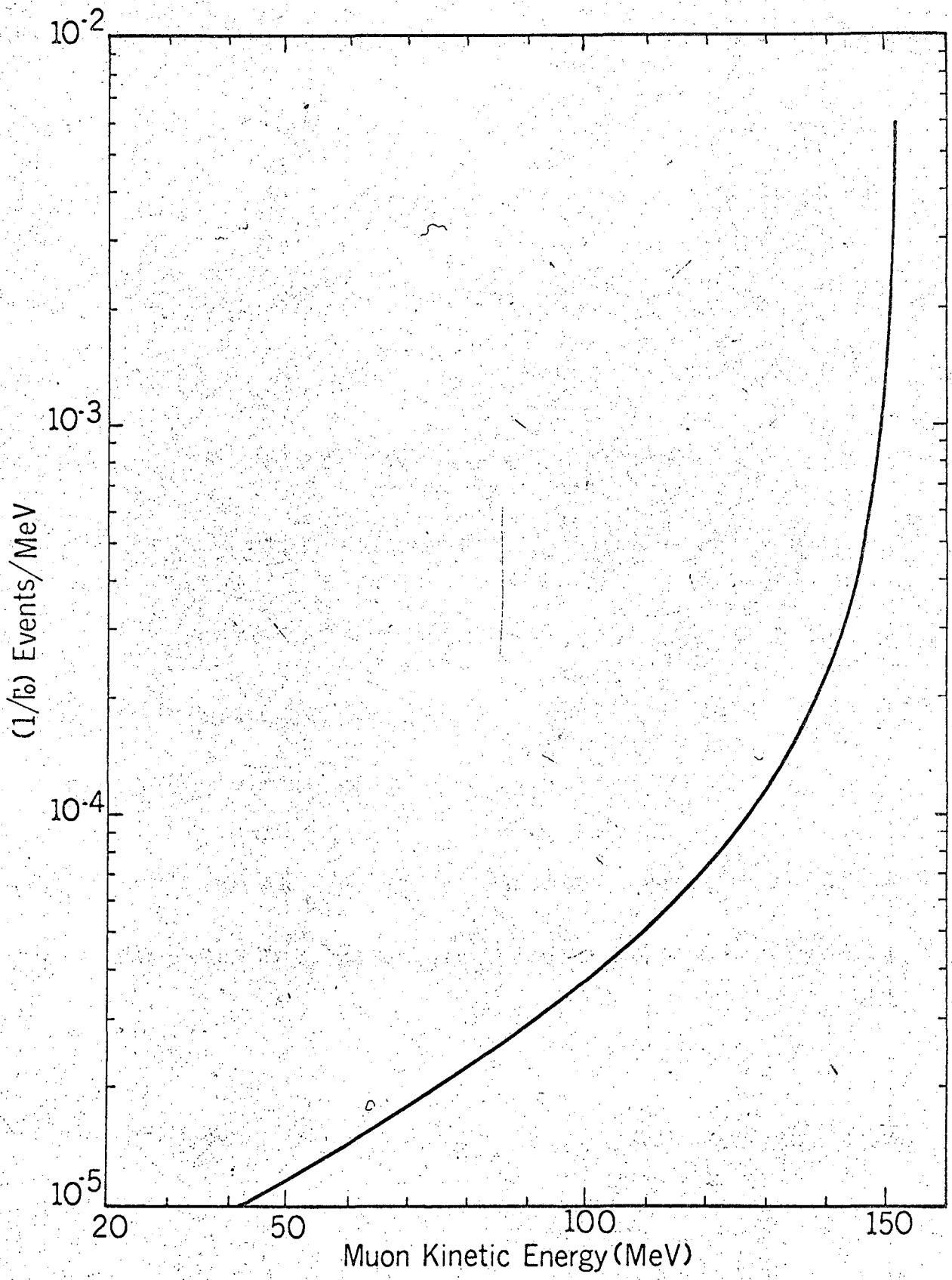
10^{-2}
10^{-3}
10^{-4}
10^{-5}
(1/fb) Events/MeV
20
50
100
150
Muon Kinetic Energy (MeV)

Fig. 6

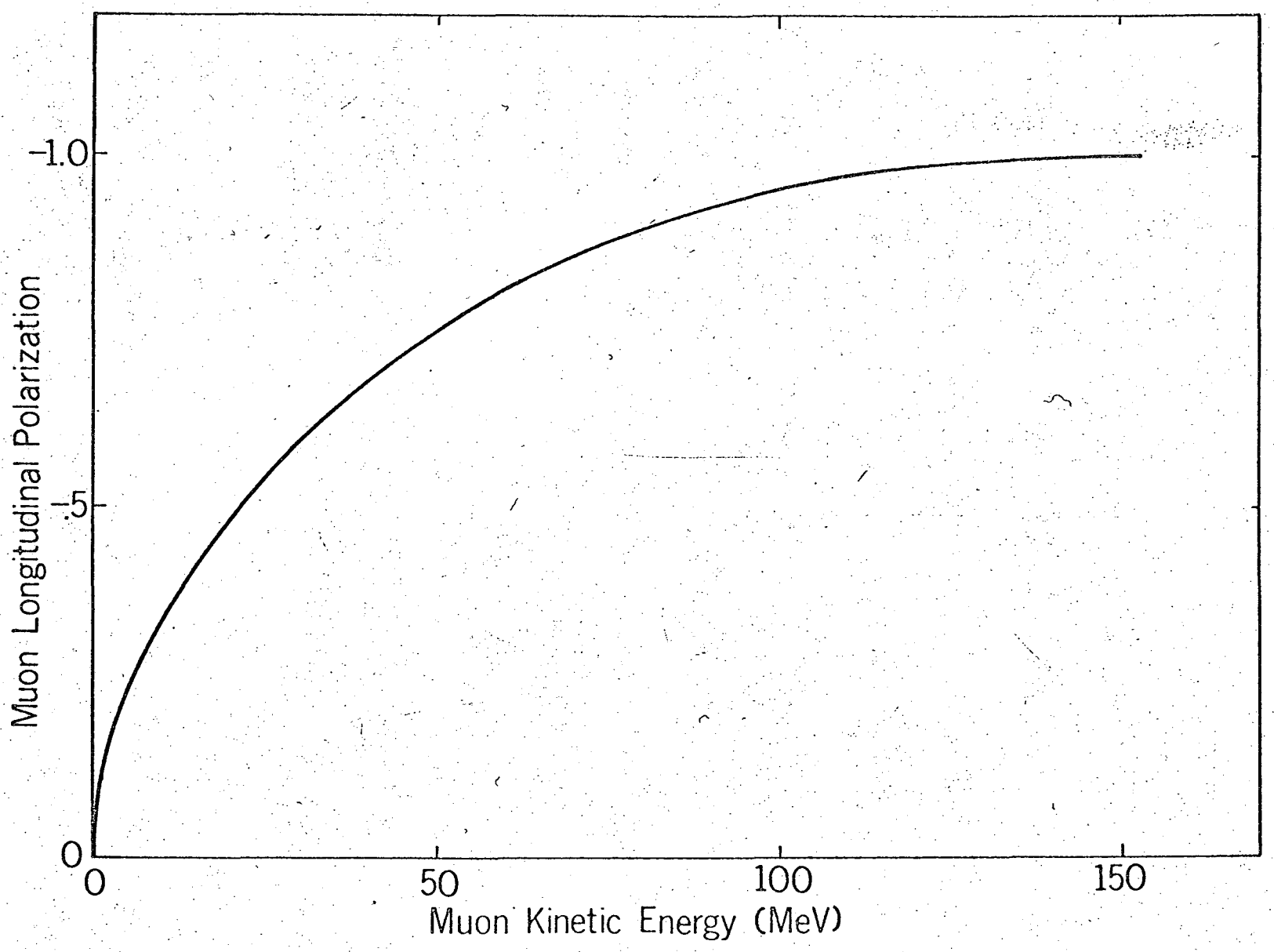
-1.0
-.5
0
Muon Longitudinal Polarization
0
50
100
150
Muon Kinetic Energy (MeV)

Fig. 7

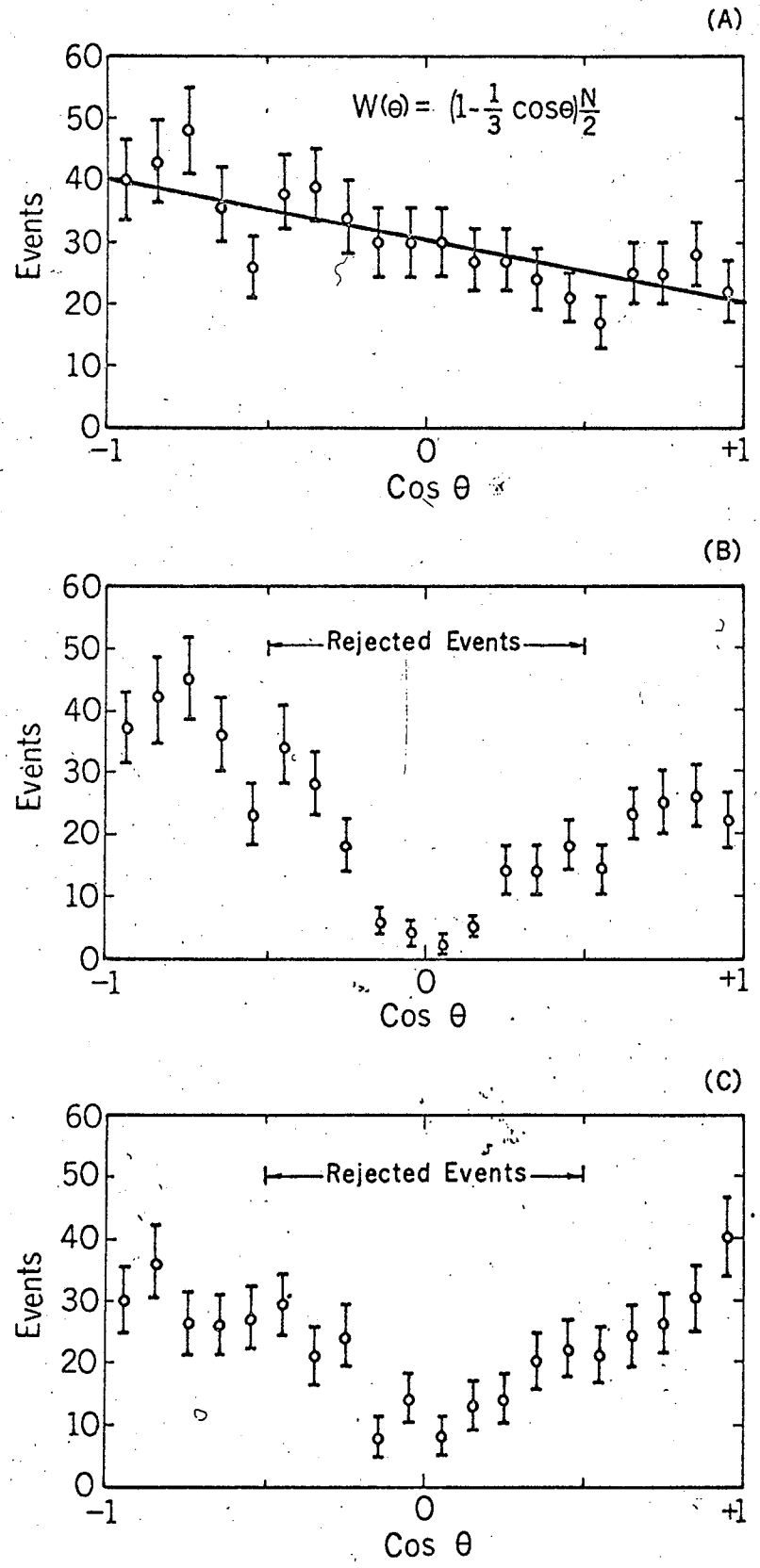
(A)
$W(\theta) = (1-\frac{1}{3}\cos\theta)\frac{N}{2}$
Events
Cos θ
(B)
Rejected Events
Events
Cos θ
(C)
Rejected Events
Events
Cos θ

Fig. 8

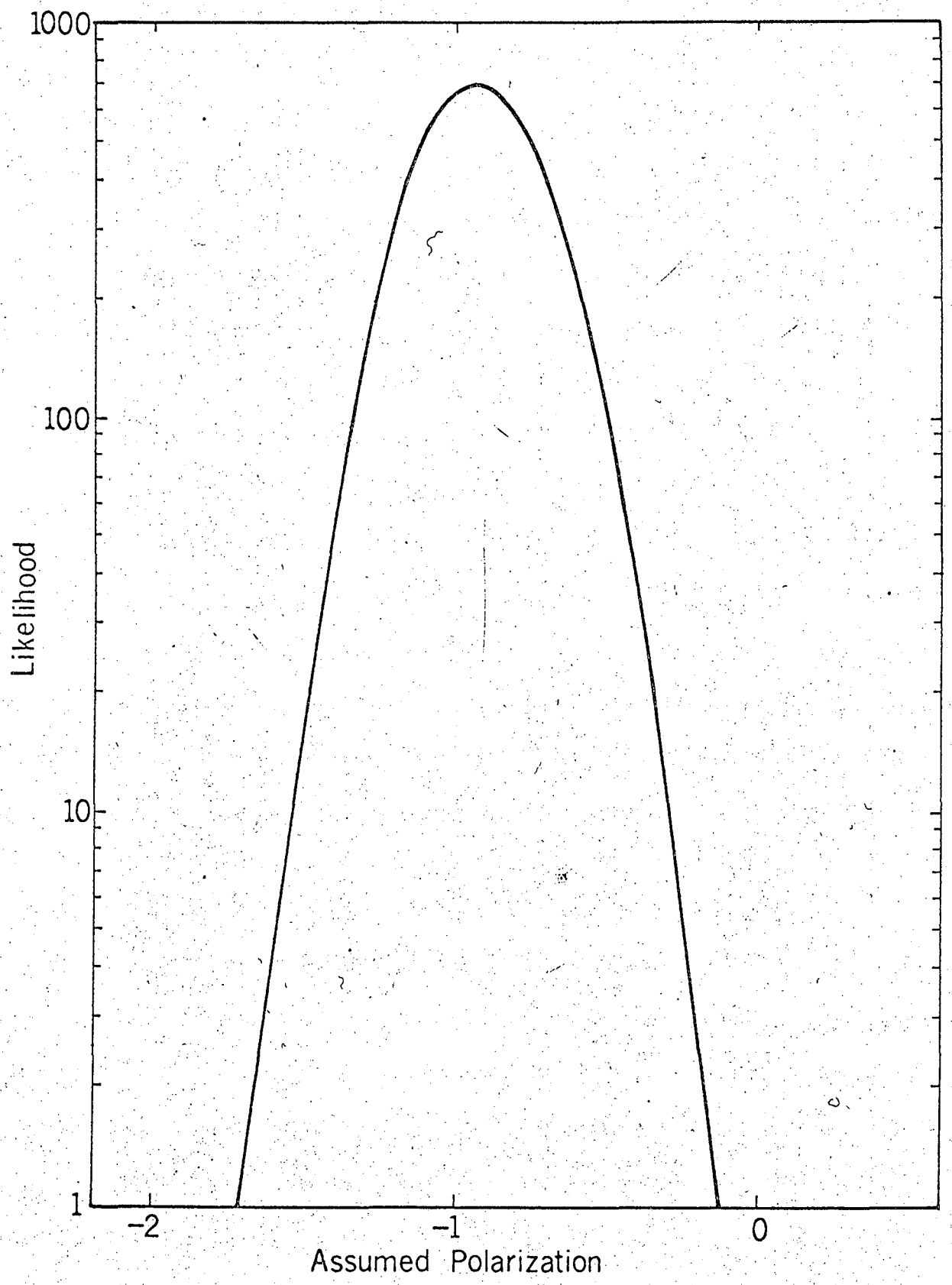

Fig. 9

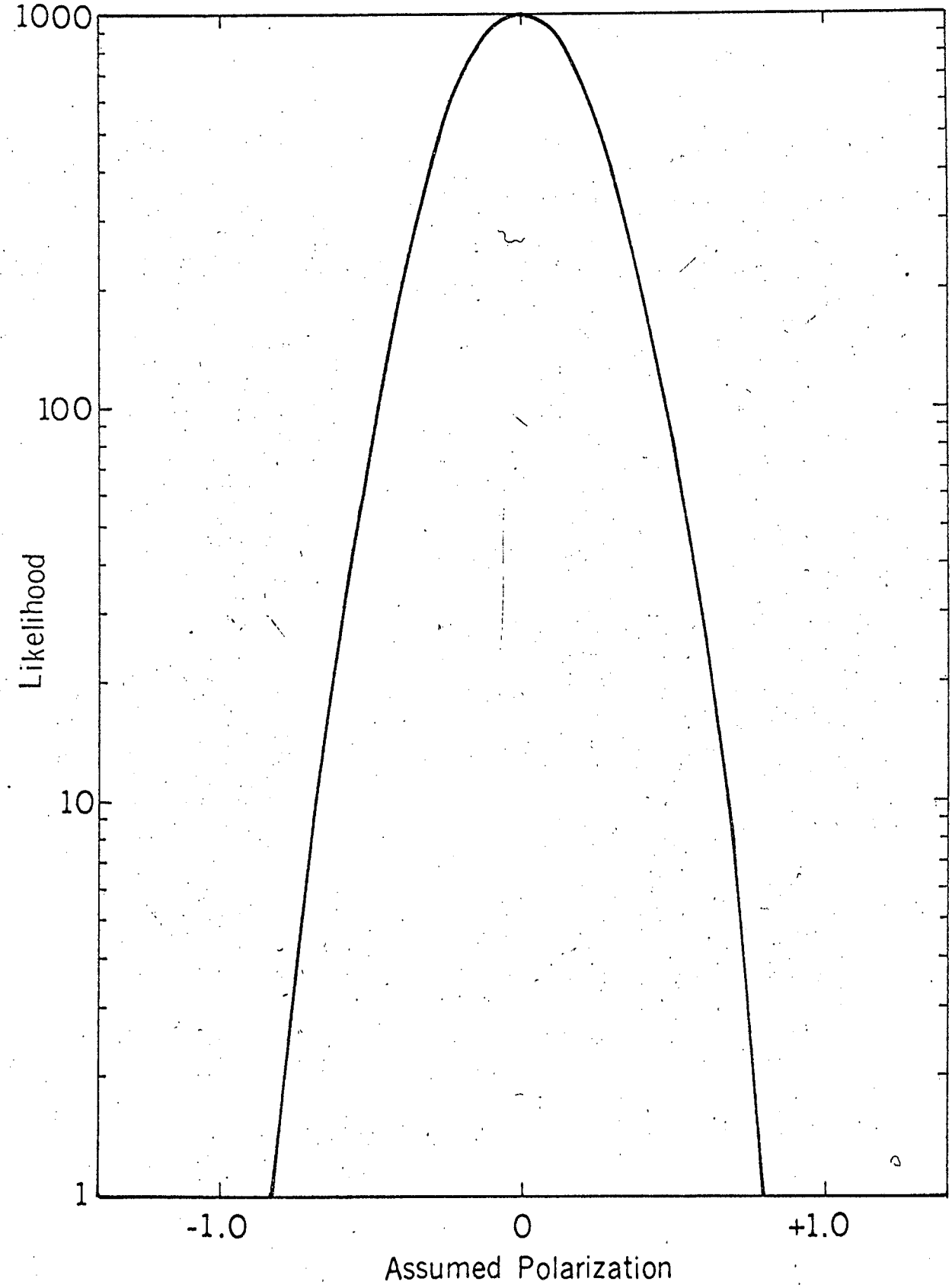

Fig. 10

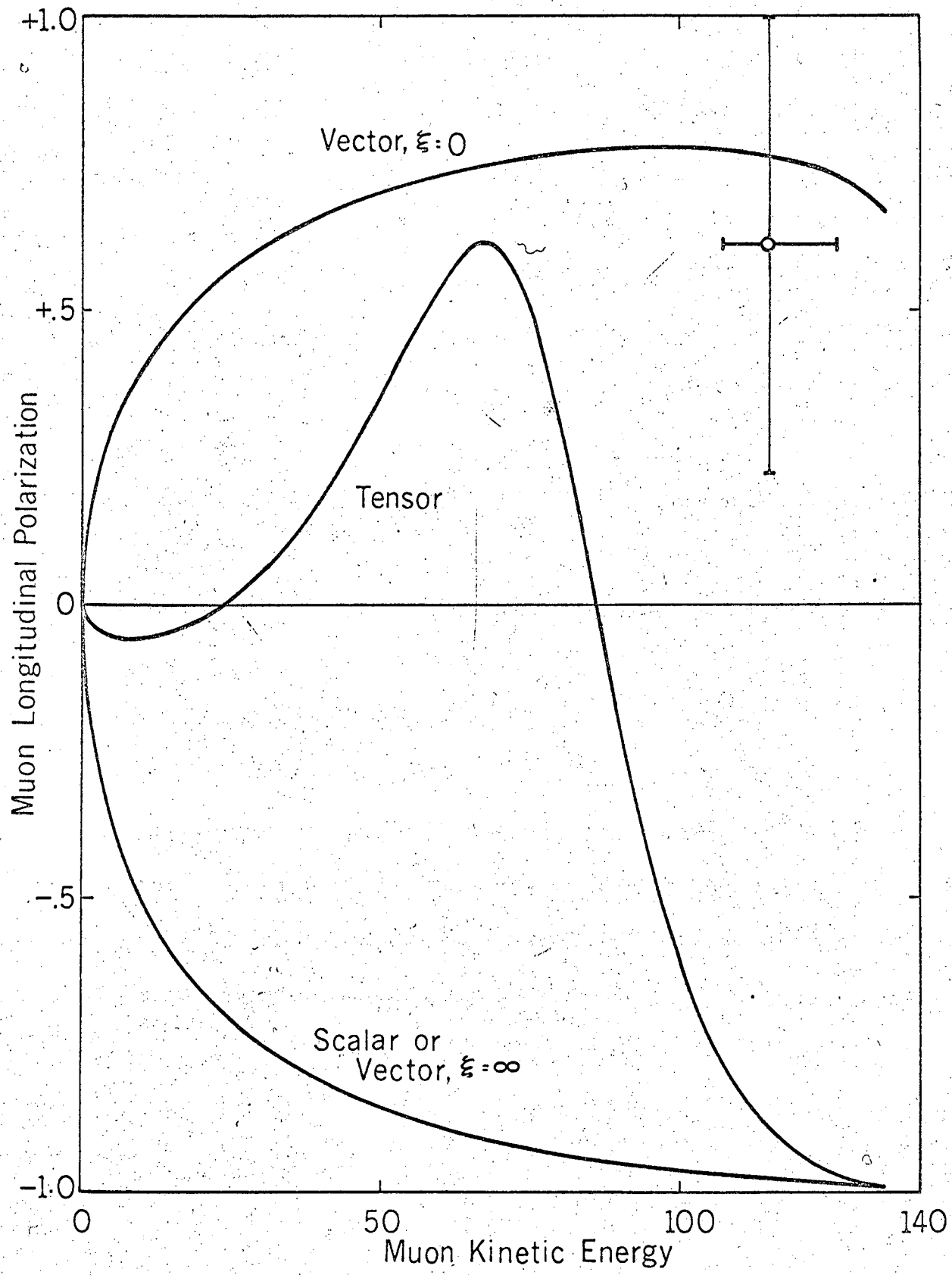
+1.0
+.5
0
-.5
-1.0
Muon Longitudinal Polarization
Vector, ξ = 0
Tensor
Scalar or
Vector, ξ = ∞
0
50
100
140
Muon Kinetic Energy

Fig. 11

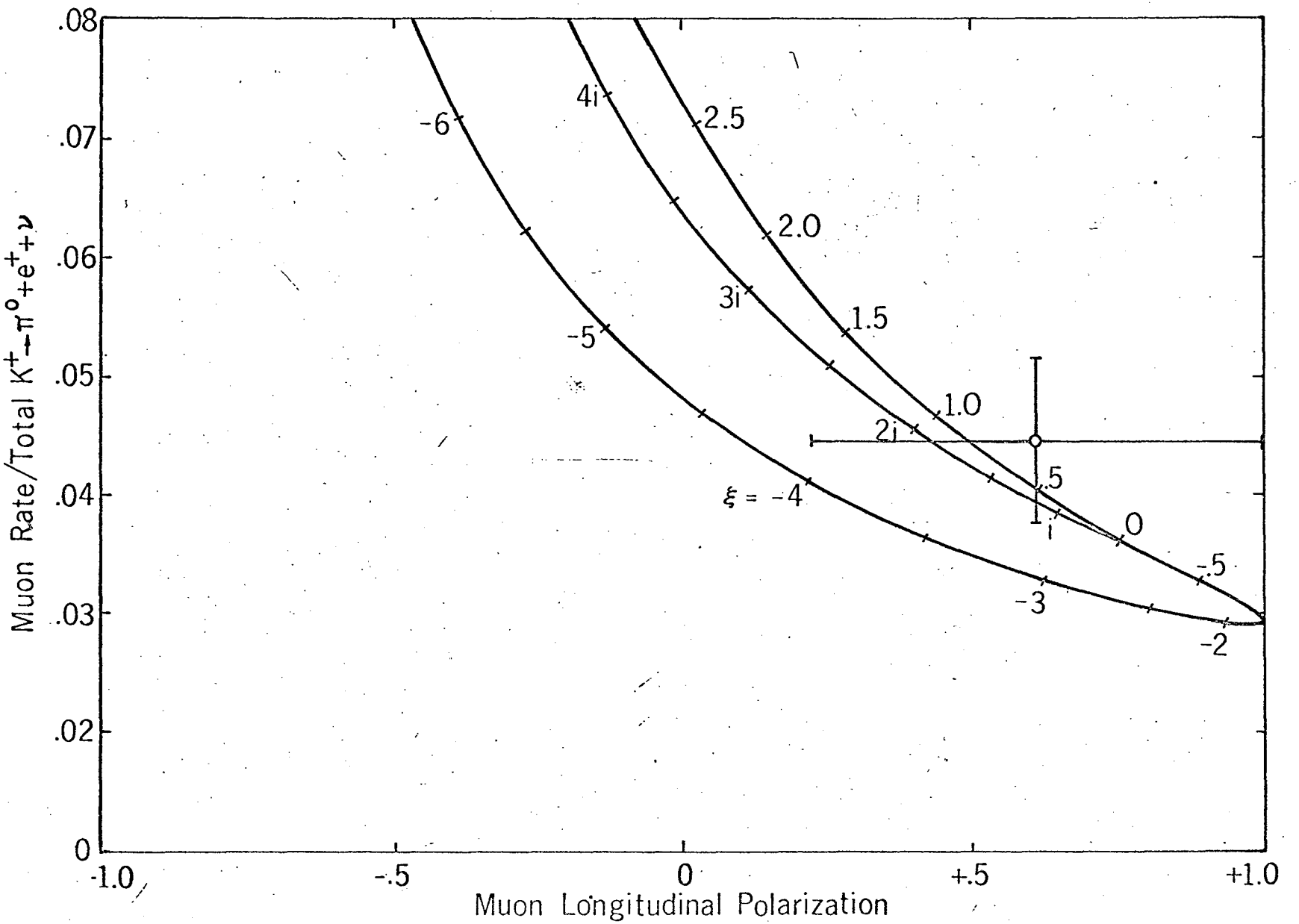
.08
.07
.06
.05
.04
.03
.02
0
-1.0
-.5
0
+.5
+1.0
Muon Rate/Total $K^+ \to \pi^0 + e^+ + \nu$
Muon Longitudinal Polarization
-6
4i
2.5
2.0
3i
1.5
-5
1.0
2i
.5
i
0
-.5
$\xi = -4$
-3
-2

Fig. 12

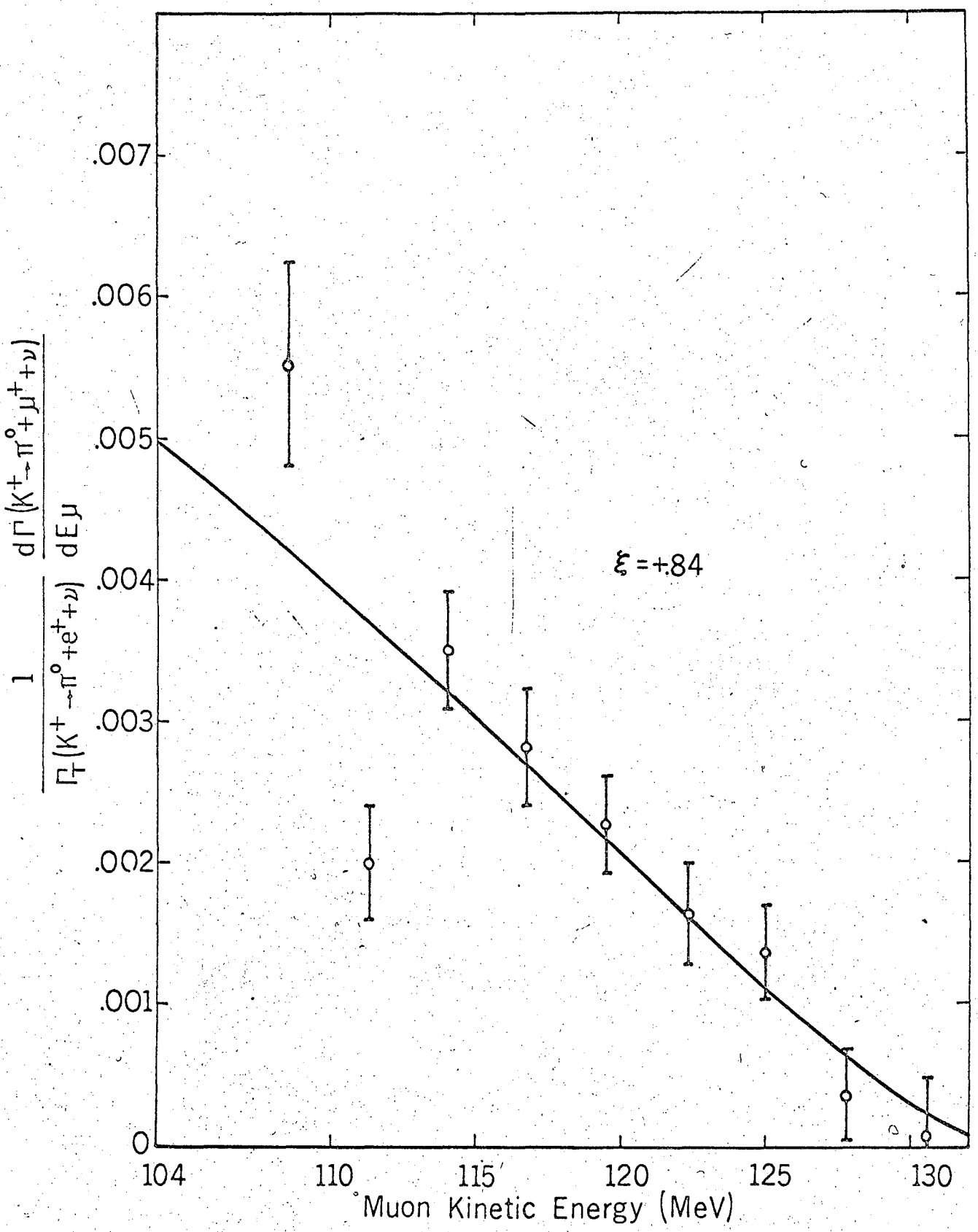
$\frac{1}{\Gamma_T(K^+ \to \pi^0 + e^+ + \nu)} \frac{d\Gamma(K^+ \to \pi^0 + \mu^+ + \nu)}{dE\mu}$
.007
.006
.005
.004
.003
.002
.001
0
$\xi = +.84$
104
110
115
120
125
130
Muon Kinetic Energy (MeV)

Fig. 13

This report was prepared as an account of Government sponsored work. Neither the United States, nor the Commission, nor any person acting on behalf of the Commission:

A. Makes any warranty or representation, expressed or implied, with respect to the accuracy, completeness, or usefulness of the information contained in this report, or that the use of any information, apparatus, method, or process disclosed in this report may not infringe privately owned rights; or

B. Assumes any liabilities with respect to the use of, or for damages resulting from the use of any information, apparatus, method, or process disclosed in this report.

As used in the above, "person acting on behalf of the Commission" includes any employee or contractor of the Commission, or employee of such contractor, to the extent that such employee or contractor of the Commission, or employee of such contractor prepares, disseminates, or provides access to, any information pursuant to his employment or contract with the Commission, or his employment with such contractor.